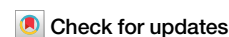


<https://doi.org/10.1038/s42004-025-01543-w>

Direct capture of a low-energy free-electron into delocalized σ^* orbitals for enabling state- and bond-selective reactions

Gorachand Das¹, Vaibhav S. Prabhudesai¹✉ & Y. Sajeev²✉

Chemically activating a bond by capturing a low-energy free-electron directly and resonantly into its σ^* orbital is conceptually simple and yet the most fascinating possibility for achieving state-specific and bond-specific chemical control. But this direct approach has not been explored experimentally due to the very low resonant electron capture cross-section of electrons into the σ^* orbital. Here we report defunctionalization and dehydrogenation reactions that are bond-selectively enabled by the direct capture of a low-energy electron into the σ^* orbital. The remarkable efficiency of these reactions can be attributed to superpositions of the σ^* orbital with its vicinal or conjugated σ_{CH}^* orbitals. The ubiquity of such quantum superpositions in molecules opens unprecedented experimental possibilities in the aspiration to control chemical reactions using low-energy free-electrons.

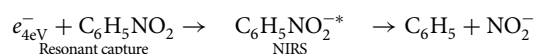
Recent advances in molecular science have made low-energy electrons (LEEs) a powerful synthetic tool for molecular transformations. Through resonant attachment to molecules, LEEs enable a realm of advanced chemical transitions originating from the corresponding electron-attached transient negative ion states, also known as negative ion resonance states (NIRS), of molecules. For instance, a unimolecular elementary reaction specific to NIRS can be initiated by simply tuning the kinetic energy of LEEs to the corresponding resonance electron attachment energy of the molecule^{1,2}. Resonant electron attachment can also be used effectively to alter the chemical reactivity of molecules and enable bimolecular reactions such as molecular association and substitution reactions^{3,4}. Resonance capture-induced chemical reactions have been extensively studied in the context of DNA damage^{5–7}. Recently, it has been demonstrated in theory and experimentation that LEE can be used as a chemical catalyst for state-specific reactions via resonant electron attachment^{8,9}.

Most remarkably, resonant electron attachment, in addition to being state-specific, is an incredible tool for site-selective chemical reactions^{1,10,11}. Site-selectivity in LEE induced reactions is a manifestation of localized NIRS. In principle, by resonantly attaching the LEE to the localized σ^* orbital, bond-selectivity—the ultimate form of site selectivity—can also be achieved. In general, defunctionalization, which involves bond breaking between a functional moiety and its parent molecule, is the simplest and most common example of a bond-selective elementary reaction step. It allows a functional group to serve as a temporary directing group in

chemical synthesis¹². Despite its conceptual simplicity, this direct approach is impractical because the localized bonding electrons of the σ -bond repel the incoming projectile electron from being captured into the σ^* orbital of the bond, making the electron capture cross-section very weak. Therefore, direct electron capture to σ^* orbitals is not a common mechanism for triggering chemical reactions, except for exceptional instances^{13–15}. In fact, the ubiquity of localized σ^* orbitals and their weak cross-section for resonant electron capture have deterred the scientific community from adequately exploring direct resonance electron attachment to various types of σ^* orbitals. Through experimental and theoretical studies of LEE-induced defunctionalization of nitrobenzene, we present here a new class of bond-selective reactions that proceed very efficiently by resonant capture of LEEs into σ^* orbitals.

Results

The LEE induced defunctionalization of nitrobenzene, which takes place around 4 eV energy of the incident electron, is a dissociative electron attachment (DEA) process, where the resonantly created NIRS of nitrobenzene unimolecularly defunctionalizes/dissociates to produce phenyl radical and nitrite ion^{16,17}.



¹Department of Nuclear and Atomic Physics, Tata Institute of Fundamental Research, Mumbai, India. ²Theoretical Chemistry Section, Bhabha Atomic Research Centre, Mumbai, India. ✉e-mail: vaibhav@tifr.res.in; sajeevy@barc.gov.in

The most significant feature of our DEA experiment is that the absolute cross-section for NO_2^- production reaches a high value of $2.45 \times 10^{-17} \text{ cm}^2$ (see Fig. 1a). Although, such a high DEA cross-section is generally observed for resonances close to 0 eV electron energy due to their vibrational Feshbach nature, such a high absolute cross-section at higher electron energies due to single particle shape resonance is particularly remarkable. It is also notably large compared to any of the other DEA channels for nitrobenzene yielding H^- , O^- , CN^- and CNO^- anions. Our experimental results in this regard are consistent with previous reports on the DEA of nitrobenzene^{16–19}. In addition, we examined the momentum images of the NO_2^- fragment, obtained for 4 eV electron energy (see Fig. 1b) by the velocity slice imaging technique²⁰. We obtained the kinetic energy distribution of this fragment as shown in figure 1c. The kinetic energy distribution of the NO_2^- fragment displays a peak at 0 eV with the highest kinetic energy around 0.5 eV, indicating that most of the fragment had minimal kinetic energy (see Fig. 1c). The unusually high cross-section for the NO_2^- anion and its low kinetic energy make the DEA channel at 4 eV intriguing, leading to further exploration. To comprehend these experimental observations, ab initio quantum chemical calculations were utilized. Figure 1d presents the computed potential energy surface for the DEA process at 4 eV.

Through our quantum chemical calculations, we have unraveled the molecular mechanism underlying this intriguing DEA process, which is surprising for multiple reasons. Typically DEA processes below 3.5 eV occur via *one-particle* NIRS generated by direct capture of LEEs to π^* orbitals, while processes above 3.5 eV occur via *two-particle one-hole* type NIRS involving electronic excitation of the target molecule^{7,15,21}. But rather unusually here at 4 eV, the NIRS participating in DEA is a *single-particle* resonance. Most unexpectedly, unlike π^* orbitals predicted for the DEA processes with high cross sections, the defunctionalization is initiated by the direct resonance capture of LEE into a σ^* orbital. This σ^* orbital, therefore, calls for careful study.

Discussion

Molecular orbital analysis in a series of functionalized benzene molecules that we consider here shows that six delocalized in-plane $\{\sigma, \sigma^*\}$ pairs of valence orbitals are formed by the superposition of twelve in-plane atomic orbitals; in-plane $2p$ orbitals from six carbon atoms, $1s$ orbitals from five hydrogen atoms, and in-plane valence orbital of the functional group (G). Among these, a $\{\sigma, \sigma^*\}$ bonding-antibonding pair results from the superposition of localized $\{\sigma_{\text{CH}}, \sigma_{\text{CH}}^*\}$ orbitals of five CH moieties and the $\{\sigma_{\text{GC}}, \sigma_{\text{GC}}^*\}$ orbital of the bond that breaks during defunctionalization determines the molecular mechanism and energetics of the DEA process (see Fig. 2).

$$\sigma_{\text{bonding}} = \sigma_{\text{GC}} + \sum_{i=2}^6 \sigma_{(\text{CH})_i}; \quad \sigma_{\text{antibonding}}^* = \sigma_{\text{GC}}^* + \sum_{i=2}^6 \sigma_{(\text{CH})_i}^* \quad (1)$$

This superposition leads to extensive delocalization of the wavefunction and stabilizes the σ orbital into an inner-valence occupied molecular orbital which is energetically much more stable than the out-of-plane π orbitals. Consequently, due to orbital splitting, the corresponding antibonding σ^* turns into an outer-valence virtual orbital and can resonantly capture a LEE of higher energy than the inner-valence π^* orbitals. All DEA processes reported here occur via the *one-particle* NIRS formed by resonant capture of a LEE in such an outer-valence σ^* orbital.

The unusually high cross-section of NO_2^- formation in the DEA process is a consequence of two efficient processes; of the highly efficient electron capture cross-section and the high electronic stability of the resulting *one-particle* NIRS. The efficient electron capture cross-section is directly attributed to the extensive delocalization of the σ^* orbital and the high intrinsic lifetime of the NIRS. Our quantum chemical calculations that utilize an in-house developed Feshbach Projection Operator Formalism²² demonstrate a significant intrinsic lifetime of $\tau \approx 10^{-13}$ s, which provides high feasibility for the reaction (see Supporting

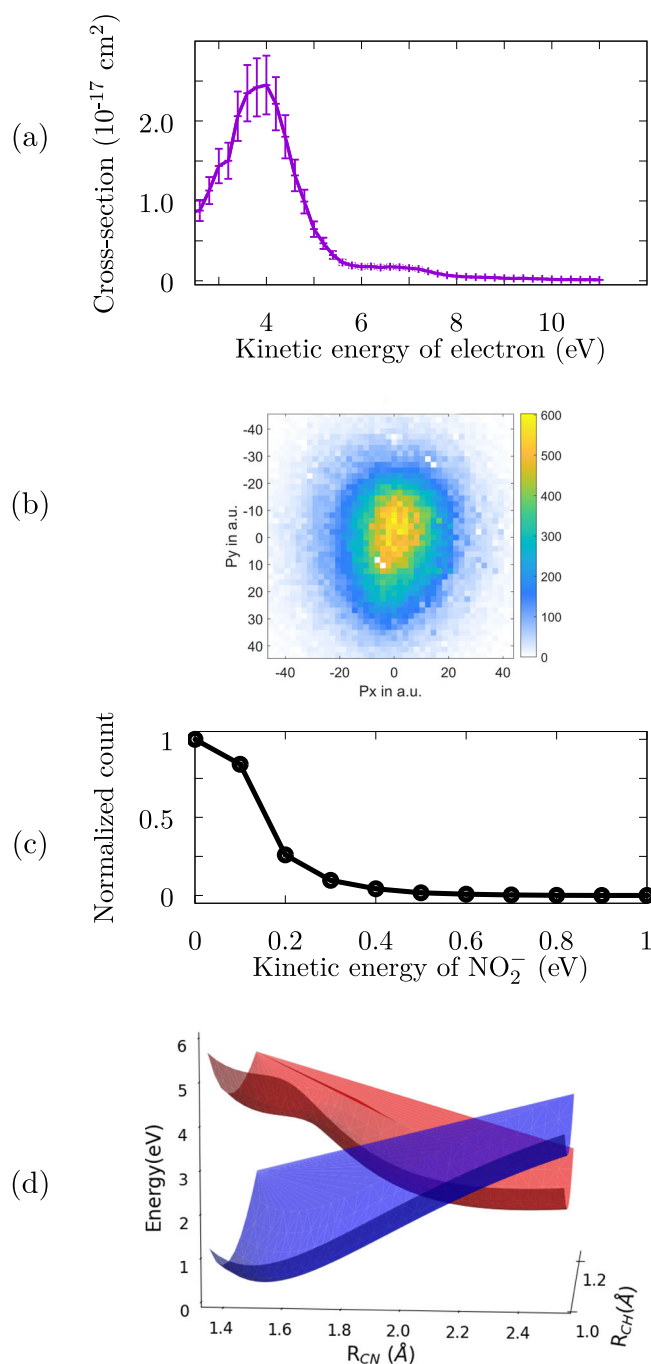


Fig. 1 | Experimental and theoretical results. **a** Absolute cross section of NO_2^- formation from DEA to nitrobenzene; **b** velocity slice image of the NO_2^- fragment at 4 eV electron energy; **c** the corresponding kinetic energy distribution obtained from the slice image; and **d** potential energy surfaces of ground state (blue) and NIRS (red).

Information). Our calculations also reveal that the NIRS state is stabilized by the large permanent dipole moment of the molecule (4.2 D), which attributes a large intrinsic lifetime to the NIRS. A similar σ^* negative ion resonance state of nitromethane that is stabilized by dipoles and effectively defunctionalizes its nitrite group has recently been reported²³. Besides dipole stabilization, the dynamic process also stabilizes the NIRS state electronically. This can also be comprehended through the extensively delocalized *one-particle* picture as explained below.

The $-\text{NO}_2$ group is a strong electron withdrawing functional group. As a result of this, the σ -electron density of the CH bonds of nitrobenzene

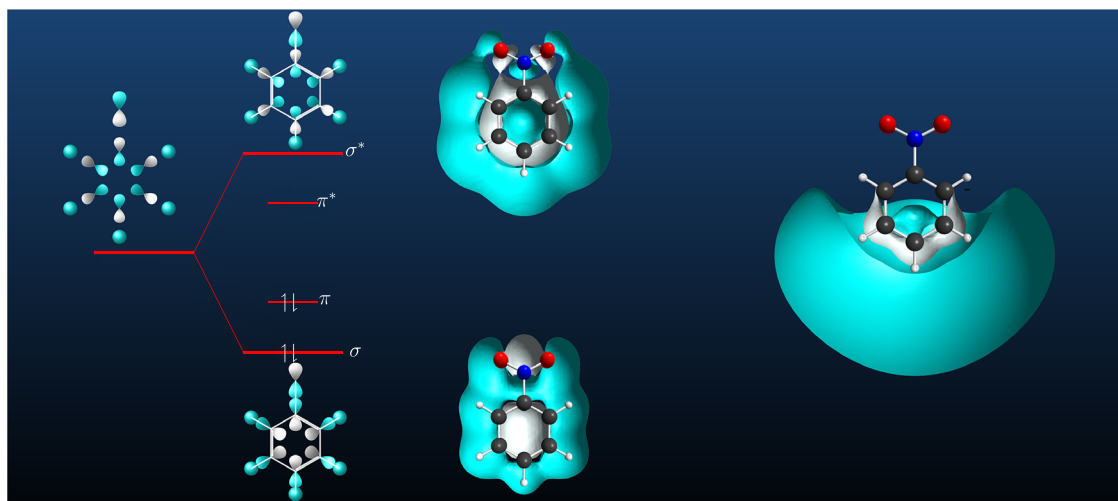


Fig. 2 | Orbitals of the one-particle σ^* NIRS. The orbital correlation diagram illustrating the formation of the in-plane inner-valence σ and the outer-valence σ^* orbital pairs from the constituent atomic orbitals of the functionalized benzene is shown on the left. The corresponding orbital pair of the nitrobenzene target state

from ab initio calculations is shown in the middle. The dipole-stabilized σ^* orbital of one-particle NIRS formed due to resonant capture of the 4 eV LEE is shown on the right.

is partially withdrawn to the NO_2 group through inductive effect. This makes all the hydrogen atoms partially positively charged. Our quantum chemical analysis shows that the hydrogen atoms together have a partial positive charge of no less than 0.5 (see Table 1). Therefore, as electron-deficient atoms, these hydrogen atoms lure the maximum electron density of the incoming LEE and localize to the σ_{CH}^* domain of the σ^* orbital. Furthermore, the H atoms, as the lightest atom, respond ultra-fast to the electron density localized in the σ_{CH}^* domain and stabilize the corresponding NIRS through the CH bond stretching. The broadening of the electron-energy-loss spectrum^{18,24,25} near 4 eV can be directly attributed to this stretching of five CH bonds (see also the discussion below). It is noteworthy that since the σ electron density does not directly respond to the out-of-plane π^* electron capture, such charge stabilization mechanism due to inductive effect may not be very significant in the case of LEE capture into π^* orbitals.

While the unusual cross-section originates from the extensive delocalization and electronic stabilization of the σ^* orbital, bond-selectivity arises from the evolution of the orbital along the DEA pathway. As the DEA progresses, the superposition that is responsible for the orbital delocalization weakens, resulting in the evolution of localized orbitals. As a result, the electron density localizes more on the σ_{CC}^* orbital, and the corresponding bond stretching, leading to defunctionalization, dictates the minimum energy path (MEP). In principle, as the direct evidence of the resonant capture of an electron into such an extensively delocalized σ^* orbital with σ_{CH}^* contributions, the electron transmission spectrum of nitrobenzene should reveal a very broad peak near 4 eV. Despite the broad peak being observed in the experiments^{18,24,25}, due to the lack of knowledge about the extensive delocalization of the σ^* orbital of nitrobenzene, the broad nature of the peak was mistakenly attributed to a core excited resonant capture that involves the excitation of the target molecule to widely diffused π^* orbital.

Table 1 | Charge analysis

| Molecules | Q_{target} | Q_{NIRS} |
|-----------------------------------|---------------------|-------------------|
| $\text{C}_6\text{H}_5\text{NO}_2$ | +0.945 (+0.672) | −0.068(+0.035) |
| $\text{C}_6\text{H}_5\text{F}$ | +1.098(+0.673) | −0.091(−0.005) |
| $\text{C}_6\text{H}_5\text{COOH}$ | +1.150(+0.680) | −0.012(+0.027) |

The sum of the Mulliken (and Löwdin) partial electric charge on all hydrogen atoms, $Q = \sum_i \delta_i^{\text{hydrogen}}$, before and after resonant capture is tabulated for the molecules in their target geometry.

The results of our quantum chemical calculations demonstrate that there are no barrierless or low-barrier DEA paths associated with core-excited negative ion resonance state near 4 eV.

Interestingly, the electronic stabilization along the MEP also accounts for the very low kinetic energy of the NO_2^- fragment. As discussed above, in the MEP of DEA yielding NO_2^- , the hydrogen atoms in the benzyl moiety are relaxed. Further, as the DEA proceeds through this MEP, the localization of the electron in the NO_2^- fragment relaxes the NO bonds. In other words, the transfer of electronic stabilization energy into intramolecular vibrational relaxation (IVR) modes of CH and NO bonds minimizes the distribution of electronic energy to the kinetic energy of the fragments. For the other molecules with high dipole moments like fluorene and benzoic acid, our calculations show the efficient defunctionalization on LEE capture to the delocalized σ^* orbital. The details of these calculations are included in the supporting information.

The direct resonant capture into delocalized σ^* orbitals can in principle allow the chemical control by selecting each bond within a molecule individually. Stabilization of the one-particle NIRS along its bond-selective reaction pathways is essential for accomplishing such bond selectivity. Dehydrogenation of the glycosidic and the non-glycosidic nitrogen moieties in thymine, labeled as N1 and N2 respectively in Fig. 3, is the first reaction to experimentally unravel the bond selectivity in resonant capture of LEEs^{1,10}. The orbital analysis presented in Fig. 3a suggests that the DEA channels at 5.5 eV and 6.8 eV, yielding H-anions from N1 and N2 sites respectively, are likely to proceed through the direct capture of an electron into the delocalized σ^* orbitals. Our quantum chemical calculations, which are summarized in Fig. 3b, c, show that these two bond-selective DEA channels indeed proceed through the resonant capture of LEEs into delocalized σ^* orbitals. The associated negative ion states are long-lived ($\tau \sim 10^{-13}$ s), making dissociation competitive over the autodetachment. While the extensive delocalization of these σ^* orbitals facilitate the electron induced chemical activation, the bond selectivity originates from the electronic stabilization of the corresponding NIRS along the respective reaction paths.

It should be noted that despite there being a ${}^2\Pi_u$ type two-particle one-hole NIRS near 6.8 eV, it is expected to have a minimal impact on the dehydrogenation of the N2 site. A major out-of-plane geometrical distortion of the ring atoms that couples ${}^2\Pi_u$ state with the dissociative Σ_u state is essential for the reaction to occur¹⁵. On the other hand, because of the superposition of localized orbitals as shown in equation (1), the higher energy non-dissociative ${}^2\Sigma_u$ NIRS surface at 6.8 eV, which is shown in green

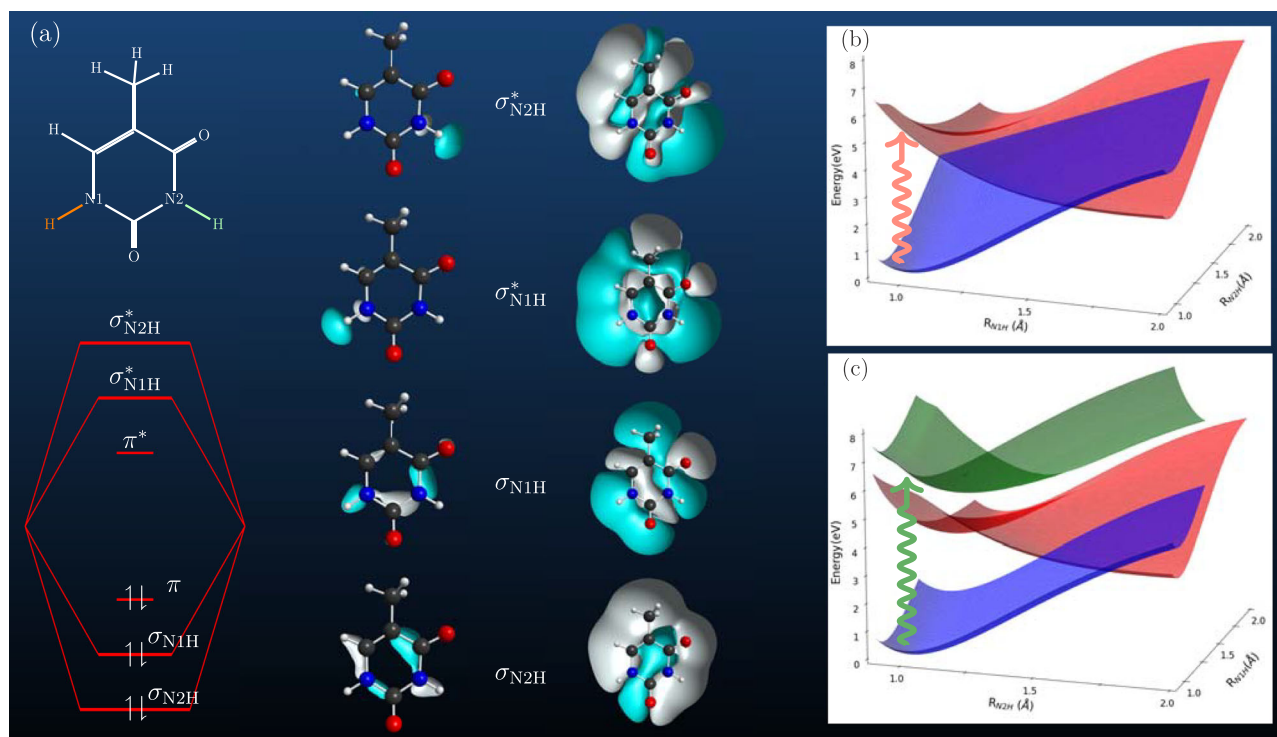


Fig. 3 | Bond-selectivity in thymine. **a** The orbital correlation diagram illustrates the energy positions of σ and σ^* orbitals. Each of these orbitals is also displayed with an iso-density surface value of 0.1 and 0.001. In **(b, c)**, the potential energy surfaces along the N1H and N2H bonds are depicted for both the ground state (blue color) and two $^2\Sigma_u$ -type *one-particle* NIRS. These two NIRS surfaces, shown in red and

green, correspond to the capture of the 5.5 eV LEE into σ_{N1H}^* orbital and the 6.8 eV LEE into σ_{N2H}^* orbital, respectively. While **(b)** demonstrates the DEA at 5.5 eV to eliminate H-anions from the N1 site, **(c)** demonstrates the DEA process at 6.8 eV to yield H-anions from the N2 site, where the resonant capture is depicted by wavy arrows.

color in Fig. 3c, is diabatically coupled to a dissociative Σ_u NIRS surface through an avoided crossing, without distorting the molecular planarity. Thus, the DEA process due to the direct σ^* capture at 6.8 eV takes place very efficiently via a MEP that connects these two surfaces.

Conclusions

To conclude, the exceptionally high DEA cross-section observed in the NO_2^- channel of nitrobenzene arises from a resonance that is long-lived against autodetachment. Our *ab initio* quantum chemical calculations reveal that this resonance is a single-particle shape resonance, with the incoming electron occupying a delocalized σ^* orbital. To the best of our knowledge, it is the first such incidence where a single particle σ^* resonance with a low autodetachment rate is directly accessed with a large capture cross-section due to its delocalized nature. Further investigation reveals the presence of similarly delocalized σ^* orbitals in a variety of chemically important molecules, highlighting the broader implications of these findings for achieving control over the chemistry of molecules using LEEs.

More broadly, this work expands the landscape of LEE-induced chemistry. As the most promising quantum tool available to shape the future of chemistry, LEEs make it possible to control the chemistry of molecular process with remarkable state-selectively and bond-selectively. The molecular domain of this chemical control, however, was restricted to π molecules because it was assumed that negative ion resonances efficiently originate only from orbitals of π molecules. Our theoretical and experimental demonstration of highly efficient bond-selective dissociation via direct resonance capture of electrons into σ^* orbitals, which were previously thought to lack chemical activity, opens the door to LEE-induced chemical control over a large domain of molecules.

Methods

Our DEA experimental setup consists of two beams that intersect at right angle, one pulsed electron beam and one molecular beam in the interaction

region of the time-of-flight (ToF) mass spectrometer²⁰. A hairpin filament is the source of the electron beam, which typically has an energy resolution of 0.8 eV. The negative ions created during the LEE-molecule interaction were pushed into the ToF mass-spectrometer using a pulsed ion extraction field. The fragment anions generated are transported to the detector at the end of the spectrometer by the electrostatic lens assembly, which has four segments. This segmentation of the ToF mass spectrometer and high-field extraction pulse ensures that all anions produced are captured irrespective of their initial kinetic energy up to 2 eV for H- and up to 5 eV for other ions up to mass 100 amu. The relative flow technique²⁶, with the O^- ions produced through DEA to O_2 as a reference, is used to determine the absolute cross-sections of the anions produced via the DEA process²⁷. When the ToF is operated in the momentum imaging mode, the kinetic energy distribution of the fragment anions is obtained using the velocity slice imaging technique. The slice images of the Newton sphere were obtained by pulsing the phosphor screen based position sensitive detector. The detector was kept active only during the 10 ns high voltage pulse. The on time of the pulse was matched with the arrival time of the central part of the Newton sphere of the fragment ions at the detector.

The molecular mechanism of the DEA processes that proceed through the *one-particle* NIRS is calculated in the following way. We chose a compact molecular basis set that describes only the valence states of a negative ion, and the discretized free-electron continuum states in the energy range we are interested in are not represented by it. In addition, the hydrogen atom basis set is scaled to achieve maximum stabilization of the NIRS. The electron-attached equation-of-motion coupled cluster singles and doubles (EA-EOMCCSD) method is utilized for computing the electronic surfaces of the NIRS, where the NIRS are obtained as bound states above the threshold for ionization of the anionic system. Since the same level of electron correlation is utilized for both the target ground state and NIRSs, the precise energy position of the resonances is obtained. Furthermore, this approach also ensures the correct

dissociation behavior of NIRS surfaces in the region of the ground state potential well. Detailed experimental and computational information can be found in the Supporting Information.

Data availability

Correspondence and the request for the data shown in the figures and other findings of this study should be addressed to V.P. (vaibhav@tifr.res.in) or Y.S. (sajeevy@barc.gov.in).

Received: 12 November 2024; Accepted: 30 April 2025;

Published online: 13 May 2025

References

1. Ptasinska, S. et al. Bond-selective H^- ion abstraction from thymine. *Angew. Chem. Int. Ed.* **44**, 1647–1650 (2005).
2. Prabhudesai, V. S., Kelkar, A. H., Nandi, D. & Krishnakumar, E. Functional group dependent site specific fragmentation of molecules by low energy electrons. *Phys. Rev. Lett.* **95**, 143202 (2005).
3. Langer, J., Matejcek, S. & Illenberger, E. The nucleophilic displacement ($sn2$) reaction $F^- + CH_3Cl \rightarrow CH_3F + Cl^-$ induced by resonant electron capture in gas phase clusters. *Phys. Chem. Phys.* **2**, 1001–1005 (2000).
4. Davis, D. & Sajeev, Y. Inducing chemical reactivity on specific sites of a molecule using the coulomb interaction exerted by a low energy electron. *Phys. Chem. Phys.* **20**, 6040–6044 (2018).
5. Boudaïffa, B., Cloutier, P., Hunting, D., Huels, M. A. & Sanche, L. Resonant formation of DNA strand breaks by low-energy (3 to 20 eV) electrons. *Science* **287**, 1658–1660 (2000).
6. Khorsandgolchin, G., Sanche, L., Cloutier, P. & Wagner, J. R. Strand breaks induced by very low energy electrons: Product analysis and mechanistic insight into the reaction with tpt. *J. Am. Chem. Soc.* **141**, 10315–10323 (2019).
7. Berdys, J., Anusiewicz, I., Skurski, P. & Simons, J. Damage to model DNA fragments from very low-energy (< 1 eV) electrons. *J. Am. Chem. Soc.* **126**, 6441–6447 (2004).
8. Davis, D., Vysotskiy, V. P., Sajeev, Y. & Cederbaum, L. S. Electron impact catalytic dissociation: Two-bond breaking by a low-energy catalytic electron. *Angew. Chem. Int. Ed.* **50**, 4119–4122 (2011).
9. Davis, D., Vysotskiy, V. P., Sajeev, Y. & Cederbaum, L. S. A one-step four-bond-breaking reaction catalyzed by an electron. *Angew. Chem. Int. Ed.* **51**, 8003–8007 (2012).
10. Ptasinska, S. et al. Bond selective dissociative electron attachment to thymine. *J. Chem. Phys.* **123**, 124302 (2005).
11. Orzol, M. et al. Bond and site selectivity in dissociative electron attachment to gas phase and condensed phase ethanol and trifluoroethanol. *Phys. Chem. Chem. Phys.* **9**, 3424 (2007).
12. Zhang, F. & Spring, D. R. Arene C–H functionalisation using a removable/modifiable or a traceless directing group strategy. *Chem. Soc. Rev.* **43**, 6906–6919 (2014).
13. Gallup, G. A. Role of a short-lived σ^* resonance in formic-acid O–H bond breaking. *Phys. Rev. A* **88**, 052705 (2013).
14. Sobczyk, M. et al. Coulomb-assisted dissociative electron attachment: application to a model peptide. *J. Phys. Chem. A* **109**, 250–258 (2004).
15. Allan, M. Measuring and modeling absolute data for electron-induced processes. *J. Phys.: Conf. Ser.* **388**, 012001 (2012).
16. Jäger, K. & Henglein, A. Negative ionen durch elektronenstoß aus organischen nitroverbindungen, Äthylnitrit und Äthylnitrat. *Z. f.ür. Naturforsch. A* **22**, 700–704 (1967).
17. Compton, R. N., Huebner, R. H., Reinhardt, P. W. & Christophorou, L. G. Threshold electron impact excitation of atoms and molecules: Detection of triplet and temporary negative ion states. *J. Chem. Phys.* **48**, 901–909 (1968).
18. Modellia, A. & Venuti, M. Empty level structure and dissociative electron attachment in gas-phase nitro derivatives. *Int. J. Mass Spectrom.* **205**, 7–16 (2001).
19. Pelc, A., Scheier, P. & Märk, T. Low-energy electron interaction with nitrobenzene: $C_6H_5NO_2$. *Vacuum* **81**, 1180–1183 (2007).
20. Das, S., Swain, S., Gope, K., Tadsare, V. & Prabhudesai, V. S. Effect of static gas background signal on momentum imaging in electron-molecule collision experiment. *Int. J. Mass Spectrom.* **498**, 117215 (2024).
21. Davis, D. & Sajeev, Y. A hitherto unknown stability of DNA basepairs. *Chem. Commun.* **56**, 14625–14628 (2020).
22. Sajeev, Y., Thodika, M. & Matsika, S. A unique QP partitioning and sievert width using real-valued continuum-remover potential. *J. Chem. Theory Comput.* **18**, 2863–2874 (2022).
23. Abdoul-Carime, H., Thiam, G. & Rabilloud, F. Production of nitrogen dioxide, no_2^- , anion from dissociative electron attachment to nitromethane below 1 eV and its temperature dependence: Direct vs dipole bound mediated processes. *J. Phys. Chem. Lett.* **15**, 10329–10333 (2024).
24. Asfandiarov, N. et al. Temporary anion states and dissociative electron attachment to nitrobenzene derivatives. *Int. J. Mass Spectrom.* **264**, 22–37 (2007).
25. Ranković, M. et al. Resonances in nitrobenzene probed by the electron attachment to neutral and by the photodetachment from anion. *J. Chem. Phys.* **157**, 064302 (2022).
26. Srivastava, S. K., Chutjian, A. & Trajmar, S. Absolute elastic differential electron scattering cross sections in the intermediate energy region. i. h_2 . *J. Chem. Phys.* **63**, 2659–2665 (1975).
27. Rapp, D. & Briglia, D. D. Total cross sections for ionization and attachment in gases by electron impact. ii. negative-ion formation. *J. Chem. Phys.* **43**, 1480–1489 (1965).

Acknowledgements

G.D. and V.P. acknowledge the financial support from the Department of Atomic Energy, India, under Project Identification No. RTI4002.

Author contributions

V.P. and G.D. planned and executed the experiments. Y.S. and G.D. planned and carried out the computations. All authors discussed the results and the conclusions were drawn. Y.S. and G.D. and V.P. wrote the manuscript and the Supporting Information.

Competing interests

The authors declare no competing interests.

Additional information

Supplementary information The online version contains supplementary material available at <https://doi.org/10.1038/s42004-025-01543-w>.

Correspondence and requests for materials should be addressed to Vaibhav S. Prabhudesai or Y. Sajeev.

Peer review information *Communications Chemistry* thanks the anonymous reviewers for their contribution to the peer review of this work. Peer reviewer reports are available.

Reprints and permissions information is available at <http://www.nature.com/reprints>

Publisher's note Springer Nature remains neutral with regard to jurisdictional claims in published maps and institutional affiliations.

Open Access This article is licensed under a Creative Commons Attribution-NonCommercial-NoDerivatives 4.0 International License, which permits any non-commercial use, sharing, distribution and reproduction in any medium or format, as long as you give appropriate credit to the original author(s) and the source, provide a link to the Creative Commons licence, and indicate if you modified the licensed material. You do not have permission under this licence to share adapted material derived from this article or parts of it. The images or other third party material in this article are included in the article's Creative Commons licence, unless indicated otherwise in a credit line to the material. If material is not included in the article's Creative Commons licence and your intended use is not permitted by statutory regulation or exceeds the permitted use, you will need to obtain permission directly from the copyright holder. To view a copy of this licence, visit <http://creativecommons.org/licenses/by-nc-nd/4.0/>.

© The Author(s) 2025